

# Amphiphilic Nanoparticles Repress Macrophage Atherogenesis: Novel Core/Shell Designs for Scavenger Receptor Targeting and Down-Regulation

Latrisha K. Petersen,<sup>†</sup> Adam W. York,<sup>†</sup> Daniel R. Lewis,<sup>‡</sup> Sonali Ahuja,<sup>†</sup> Kathryn E. Uhrich,<sup>§</sup> Robert K. Prud'homme,<sup>||</sup> and Prabhas V. Moghe<sup>\*,†,‡</sup>

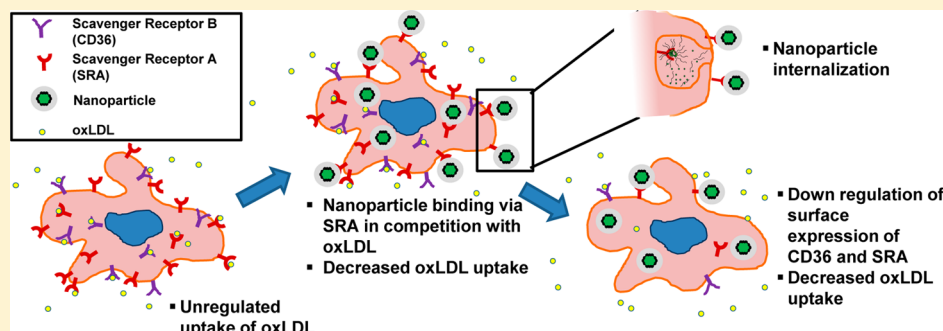
<sup>†</sup>Department of Biomedical Engineering, Rutgers University, 599 Taylor Road, Piscataway, New Jersey 08854, United States

<sup>‡</sup>Department of Chemical & Biochemical Engineering, Rutgers University, 98 Brett Road, Piscataway, New Jersey 08854, United States

<sup>§</sup>Department of Chemistry and Chemical Biology, Rutgers University, 610 Taylor Road, Piscataway, New Jersey 08854, United States

<sup>||</sup>Department of Chemical and Biological Engineering, Princeton University, Princeton, New Jersey 08544, United States

## S Supporting Information



**ABSTRACT:** Atherosclerosis, an inflammatory lipid-rich plaque disease is perpetuated by the unregulated scavenger-receptor-mediated uptake of oxidized lipoproteins (oxLDL) in macrophages. Current treatments lack the ability to directly inhibit oxLDL accumulation and foam cell conversion within diseased arteries. In this work, we harness nanotechnology to design and fabricate a new class of nanoparticles (NPs) based on hydrophobic mucic acid cores and amphiphilic shells with the ability to inhibit the uncontrolled uptake of modified lipids in human macrophages. Our results indicate that tailored NP core and shell formulations repress oxLDL internalization via dual complementary mechanisms. Specifically, the most atheroprotective molecules in the NP cores competitively reduced NP-mediated uptake to scavenger receptor A (SRA) and also down-regulated the surface expression of SRA and CD36. Thus, nanoparticles can be designed to switch activated, lipid-scavenging macrophages to antiatherogenic phenotypes, which could be the basis for future antiatherosclerotic therapeutics.

**KEYWORDS:** atherosclerosis, amphiphilic macromolecules, scavenger receptor, nanoparticle, macrophages, atherogenesis, oxidized lipoproteins

## INTRODUCTION

Atherosclerosis, defined by persistent inflammation and the buildup of lipid-rich plaques in arterial walls, leads to life threatening cardiovascular conditions such as myocardial infarction, chronic stable angina, and stroke.<sup>1</sup> This inflammation is triggered by high levels of deposited oxidized low density lipoproteins (oxLDL) within arterial walls and contributes to the formation of foam cells, the major constituent of arterial plaque growth. It is well-known that the unregulated cellular uptake of oxLDL by intimal macrophages is primarily mediated through scavenger receptors.<sup>2–6</sup> This cycle is self-perpetuated through unregulated scavenger receptor replenishment and oxLDL uptake.<sup>4</sup> Therefore, new bioactive molecules that can effectively intervene in the uptake of oxLDL via scavenger receptors in a sustained manner can offer a rational approach to

manage atherosclerosis and can present potential therapeutic targets for drug discovery.<sup>7–9</sup>

Our laboratories have proposed amphiphilic macromolecules (AMs) that competitively bind to cells via scavenger receptors and demonstrate the ability to inhibit uptake of oxLDL in IC21 macrophages,<sup>10,11</sup> THP-1 monocytes,<sup>12–15</sup> and cell lines engineered with scavenger receptors.<sup>16</sup> The chemical makeup of these AMs comprises a sugar backbone that has been acylated with lauroyl chloride followed by conjugation to 5 kDa

Received: March 8, 2014

Revised: June 25, 2014

Accepted: June 27, 2014

Published: June 27, 2014

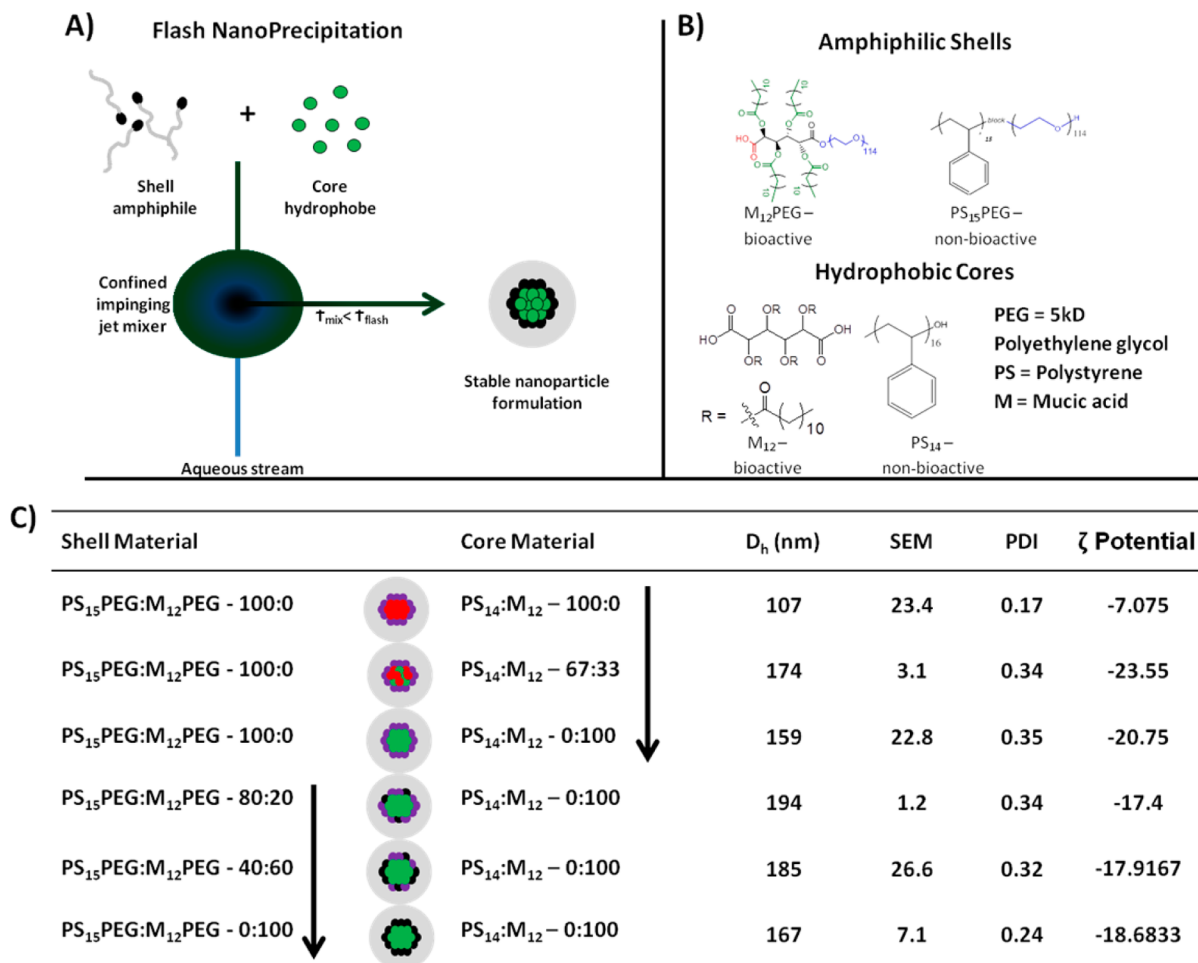


**Figure 1.** Schematic of the flash nanoprecipitation process used to fabricate kinetically assembled nanoparticles (NPs) and the resultant library of amphiphilic shell and hydrophobic core macromolecules. (A) To form colloidal stable NPs, complete homogeneous mixing between the solvent (THF) and aqueous streams must be achieved. This mixing time is represented by  $\tau_{\text{mix}}$  and the NP formation time is represented by  $\tau_{\text{flash}}$ . (B) Structures and corresponding acronyms of amphiphilic macromolecule (AM) shell and hydrophobic core components used in the formulation of NPs. (C) Table of NP composition including the core and shell materials as well as characterization including hydrodynamic diameters ( $D_h$ ), standard error of the mean (SEM) of the  $D_h$  ( $n = 2$ ), polydispersity index (PDI), and  $\zeta$  potential as measured by dynamic light scattering.

poly(ethylene glycol) (PEG). Recently, a study was conducted in which the AM micellar assemblies carrying a cholesterol efflux drug were administered to injured carotid arteries of Sprague–Dawley rats fed a high fat diet.<sup>12</sup> The localized AMs were able to inhibit macrophage retention and decrease cholesterol accumulation in the intima.

Although thermodynamically assembled micelles are promising for the delivery of water insoluble therapeutics,<sup>17–19</sup> such assemblies are vulnerable to disruption (i.e., micelle dissolution) when introduced into a physiological environment.<sup>20,21</sup> Since micelles are in a constant dynamic equilibrium between the assembled state and unimers (single macromolecules) this can lead to poor drug retention allowing the encapsulated drug and/or unimer to partition into neighboring plasma proteins or lipophilic sinks.<sup>19,22–27</sup> To overcome these challenges, our lab developed AM-based organic nanoparticles, composed of hydrophobic solutes, using a kinetic process known as flash nanoprecipitation (FNP).<sup>28–33</sup> NPs fabricated under this method are resistant to the thermodynamic instabilities of unimer partitioning that are typically associated with thermodynamic micellar formulations. Notably, the NPs composed of an AM shell/corona and a hydrophobically modified mucic acid core (M<sub>12</sub>) have shown the ability to

inhibit oxLDL uptake in human monocyte-derived macrophages (HMDMs), even in the presence of 20% serum, where analogous micellar assemblies were ineffective at that serum concentration.<sup>34</sup>

Despite the promise of the AM-based nanoparticles, the antiatherogenic mechanism of action of the NPs remains to be elucidated. Thus, the focus of this work was to utilize bioactive, serum-stable AM-derived NPs and identify the critical macromolecular determinants for regulation of scavenger-receptor-mediated mechanisms of foam cell formation and atherosclerosis. While prevalent pharmacologic factors, such as statins, aim to systematically inhibit the synthesis of cholesterol, approaches capable of managing atherosclerosis through the regulation of scavenger receptor expression may be a more lesion-directed, disease-specific treatment strategy. Insights from our studies indicate that the amphiphilic macromolecule-based nanoparticles have a potent effect not only on competitively inhibiting oxLDL uptake but also switching macrophages to a more inherently antiatherogenic phenotype.

## EXPERIMENTAL SECTION

**Materials.** Synthesis of the AMs and of the mucic acid modified with lauroyl chloride (M<sub>12</sub>) was followed as described

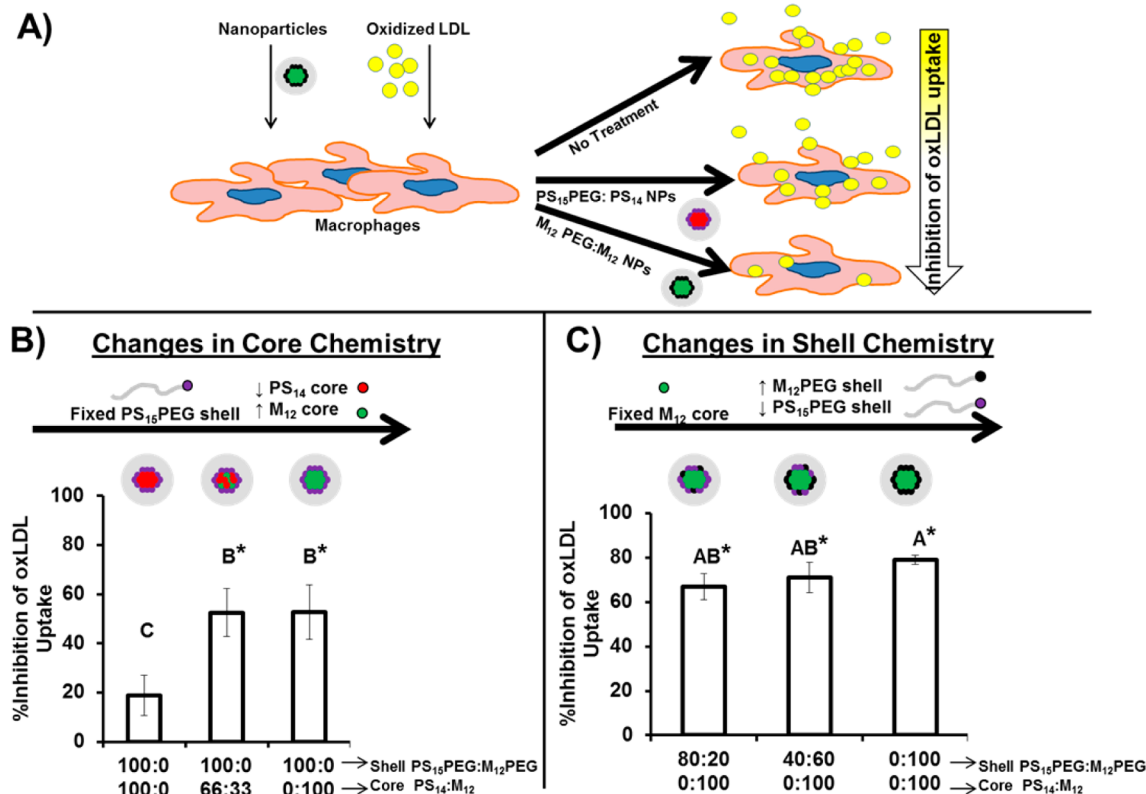


**Figure 2.** Roles of core versus shell components of the NPs on antiatherogenic activity were elucidated. (A) Schematic showing the experimental design of cultured HMDMs treated with oxLDL and different NP formulations and then assessed for the ability of the NPs to inhibit uptake of the modified LDL. (B,C) The NP shell and core contribute differentially to oxLDL uptake inhibition, wherein the “bioactive” core had a more pronounced effect. The data were acquired by flow cytometry analysis of HMDMs. (B) NPs with varying core chemistry are composed of a fixed 100% nonbioactive PS<sub>15</sub>PEG<sub>114</sub> shell formulated with differing core combinations of bioactive M<sub>12</sub> and nonbioactive PS<sub>14</sub>. (C) NPs changing in the shell chemistry and composed of a fixed 100% bioactive M<sub>12</sub> core formulated with differing shell combinations of M<sub>12</sub>PEG and nonbioactive PS<sub>15</sub>PEG<sub>114</sub>. Data are from  $n = 3$  experiments (error bars =  $\pm$ SEM). OxLDL uptake by HMDMs was evaluated after 24 h co-incubation of oxLDL (5  $\mu$ g/mL) and NPs ( $1.5 \times 10^{-5}$  M) in 10% FBS. (B,C) Statistical analysis was conducted over the entire data presented in these parts of this figure so comparisons can be made between all NP groups. Treatments with the same letter are not statistically significant from one another, and the asterisk (\*) indicates statistical significance from the oxLDL control. Statistical significance corresponds to  $p \leq 0.05$ .

previously.<sup>8,29</sup> Materials used for NP fabrication include tetrahydrofuran (THF) (Sigma-Aldrich), copolymer poly(styrene<sub>15</sub>-block-ethylene glycol<sub>114</sub>) (PS<sub>15</sub>PEG;  $M_n = 6600$  g/mol, PDI = 1.10) (Polymer Source), homopolymer polystyrene (PS<sub>14</sub>;  $M_n = 1500$  g/mol) was prepared as described previously,<sup>35</sup> and the hydrophobic fluorophore 2,2,10,10-tetraethyl-6,14-bis(triisopropylsilyl ethynyl)-1,3,9,11-tetraoxa-dicyclopenta pentacene (EtTP-5) was gifted by Prof. John Anthony from the University of Kentucky, Department of Chemistry (Lexington, KY). Cell culture, blocking assay, flow cytometry, and immunocytochemistry materials include human buffy coats (The Blood Center of NJ), macrophage colony stimulating factor (M-CSF) (PeproTech), RPMI-1640 (ATCC), penicillin/streptomycin (Lonza), Ficoll-Paque premium 1.077 g/mL (GE Healthcare), FBS and Hoechst 33342 (Life Technologies), 3,3'-dioctadecyloxacarbocyanine (DiO) labeled oxLDL (Kalen Biomedical), and unlabeled oxidized LDL (Biomedical Technologies Inc.).

**Nanoparticle Fabrication and Characterization.** Nanoparticles were fabricated via a flash nanoprecipitation process (Figure 1A) described previously.<sup>29</sup> Briefly, the shell material, either 100% AM or a combination of M<sub>12</sub>PEG and PS<sub>15</sub>PEG, were dissolved in THF at 40 mg/mL and the core material, M<sub>12</sub> and/or PS<sub>14</sub>, were dissolved at 20 mg/mL, to result in a shell to core weight ratio of 2:1. Five hundred microliters of the THF

stream was mixed with 700  $\mu$ L of the aqueous stream via a confined impinging jet mixer, after which the stream was immediately dispersed into 3.8 mL of picopure water. The NPs were dialyzed 2X against picopure water for removal of the THF. Fluorescent NPs were fabricated by coprecipitating 2.5 wt % core ETtP5 (2,2,10,10-tetraethyl-6,14-bis(triisopropylsilyl ethynyl)-1,3,9,11-tetraoxa-dicyclopenta[b,m]-pentacene)<sup>36</sup> with 97.5 wt % core (M<sub>12</sub> and/or PS<sub>14</sub>). Following dialysis, the NPs were characterized by dynamic light scattering (DLS) using a Malvern-Zetasizer Nano Series DLS detector with a 22 mW He-Ne laser operating at  $\lambda = 632.8$  nm using general purpose resolution mode. Hydrodynamic diameters (peak size from intensity distribution), and polydispersity indices (PDI) were obtained by diluting the NPs 10-fold in picopure water (Figure 1C). The structures of the different amphiphilic shells and hydrophobic cores used for NP fabrication can be found in Figure 1B.

**Peripheral Blood Mononuclear Cell Isolation and Culture.** Peripheral blood mononuclear cells (PBMCs) were isolated from human buffy coats by Ficoll-Paque (1.077 g/mL) density gradient and ACK lysis of red blood cells as described previously.<sup>29</sup> Cells were washed in PBS, centrifuged at 300g to remove platelets, and added to BD Falcon T175 flasks at a concentration of 2.85 million cells/mL in base media (RPMI 1640 supplemented with 10% FBS and 1% penicillin/

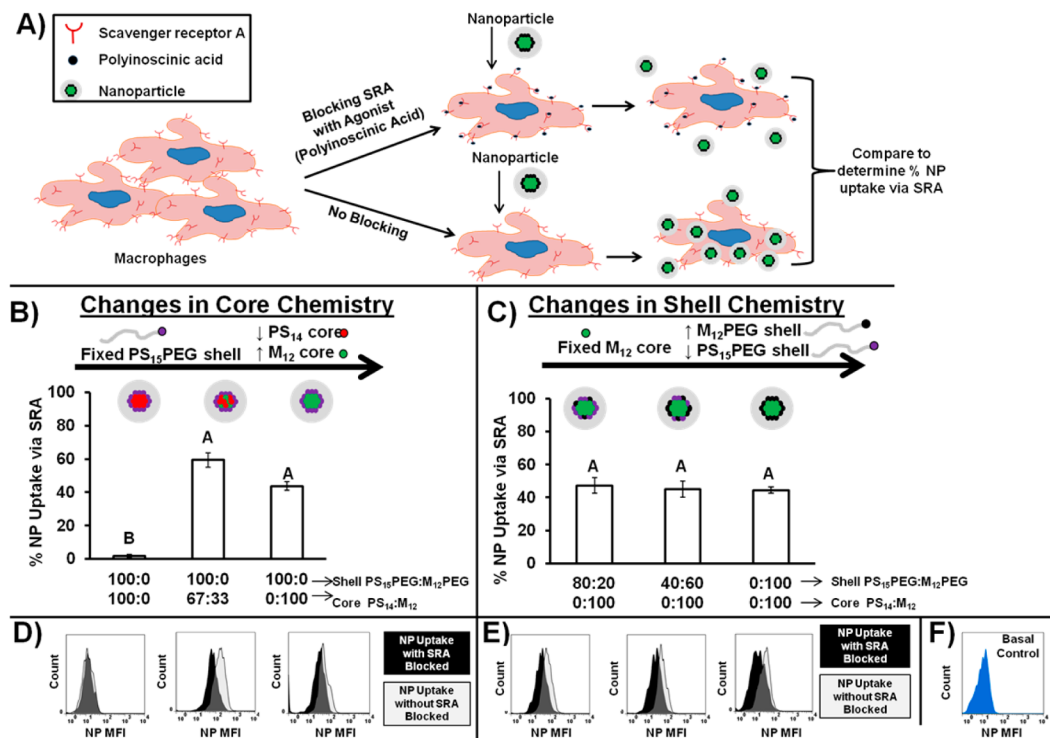


**Figure 3.** Scavenger receptor A (SRA) mediated NP uptake was dictated primarily by the M<sub>12</sub> NP core. All M<sub>12</sub> core containing NPs resulted in the highest level of NP uptake, which was confirmed to be via SRA. Minimal NP uptake was observed with the NP formulation with the PS<sub>14</sub> core. (B–E) NP association with HMDMs and (F) the basal control were obtained by flow cytometry. (A) NP uptake, determined in panels B–E, was evaluated in HMDMs after a 1 h preblocking step with polyinosinic acid and a subsequent incubation with fluorescent NPs ( $1.5 \times 10^{-5}$  M) for 6 h in the presence of 10% FBS. Percent NP uptake via SRA was determined by comparing the HMDM mean fluorescence intensity (MFI) of the NP MFI with and without SRA blocking. (B,D) NPs changing in the core chemistry are composed of a fixed 100% nonbioactive PS<sub>15</sub>PEG<sub>114</sub> shell formulated with differing core combinations of bioactive M<sub>12</sub> and nonbioactive PS<sub>14</sub>. (C,E) NPs changing in the shell chemistry and composed of a fixed 100% bioactive M<sub>12</sub> core formulated with differing shell combinations of M<sub>12</sub>PEG and nonbioactive PS<sub>15</sub>PEG<sub>114</sub>. (D–F) Representative histograms of HMDM NP MFI (x-axis) vs count (y-axis) with (black) and without (light gray) SRA blocking and basal control (blue). (B,C) Statistical analysis was conducted over the entire data presented in these parts of this figure so comparisons can be made between all NP groups. Data is from a minimum  $n = 3$  (error bars =  $\pm$ SEM). Treatments with the same letter are not statistically significant from one another and statistical significance corresponds to  $p \leq 0.05$ .

streptomycin). After 24 h of incubation at 37 °C and 5% CO<sub>2</sub>, adherent cells were selected and incubated for an additional 7 days in the base media containing 50 ng/mL M-CSF for differentiation into HMDMs. Next, cells were plated into the desired well plate (flow cytometry) or Labtek chamber (microscopy imaging) at a concentration of 150,000 cells/mL and allowed to rest for 24 h before the addition of treatments.

**OxLDL Uptake.** To evaluate the influence of NPs on oxLDL uptake, HMDMs were incubated with fluorescent DiO oxLDL (1 µg/mL, Kalen Biomedical) and unlabeled oxLDL (4 µg/mL, Biomedical Technologies) with or without NPs ( $1.5 \times 10^{-5}$  M) of each chemistry in base media for 24 h (Figure 2A). Oxidized LDL with a relative electrophoretic mobility between 1.8 and 2.1 was chosen for these studies as it correlates to a mild to high level of oxidation and is representative of the highly oxidative states of LDL encountered by macrophages in developing plaques.<sup>37</sup> Next, the cells were prepared for analysis on the flow cytometer as described in the scavenger receptor blocking assay. DiO oxLDL fluorescence was quantified via flow cytometry with a FACSCalibur (Becton Dickinson) by collecting 10,000 events per sample and analyzed with Flow Jo software (Treestar) by quantifying the DiO oxLDL MFI. A minimum of three experimental replicates was conducted for this study. Data is presented as % inhibition of oxLDL uptake and determined by the following equation:

$$\frac{\text{DiO oxLDL MFI of treatment sample}}{\text{DiO oxLDL MFI of oxLDL only control sample}} \times 100 - 100$$

**Scavenger Receptor-Mediated NP Uptake.** To evaluate the influence of blocking agents on NP uptake, HMDMs were incubated with polyinosinic acid (10 µg/mL, Sigma-Aldrich) or CD36 monoclonal antibody (2 µg/mL, clone JC63.1, Cayman Chemical) in base media for 1 h at 37 °C. The corresponding isotype control to human CD36 monoclonal antibody, purified mouse IgA, κ (BD Pharmingen, clone M18-254) was included in this experimental protocol to test for nonspecific antibody binding. Following the incubation, blocking agents were removed, cells washed, and then incubated with fluorescent NPs ( $1.5 \times 10^{-5}$  M, 2.5 wt % core ETtPS with 97.5 wt % core M<sub>12</sub>) of distinct compositions for 6 h (Figure 3A). Next, the cells were prepared for flow cytometry by washing and then incubation with 2 mM EDTA for 15 min on cold packs. After vigorously pipetting each sample the cells were transferred to 5 mL polystyrene tubes, centrifuged at 1000 rpm for 10 min, and then fixed with 1% paraformaldehyde (PFA). NP fluorescence was quantified via flow cytometry with a FACSCalibur (Becton Dickinson) by collecting 10,000 events per sample and analyzed with Flow Jo software (Treestar) by quantifying the

NP mean fluorescence intensity (MFI) of the HMDM population. A minimum of three experimental replicates was conducted for this study. The degree of inhibition of NP uptake caused by each blocking agent was determined by the following equation:

$$\% \text{NP uptake} = 100 \times \frac{\text{NP MFI sample pretreated with blocking agent}}{\text{NP MFI sample not pretreated with blocking agent}}$$

**Scavenger Receptor Surface Expression.** To evaluate the influence of NPs on cell surface scavenger receptor expression, HMDMs were incubated with unlabeled oxLDL (5 µg/mL) with or without NPs of each chemistry for 24 h. Following the incubation, treatments were removed, and cells were prepared for evaluation via flow cytometry or microscopy. For flow cytometry preparation, the cells were washed in blocking buffer (0.5% bovine serum albumin (BSA), 0.1% sodium azide, and 1% normal goat serum in PBS), and incubated with 2 mM EDTA diluted in blocking buffer for 15 min on cold packs. After vigorously pipetting each sample they were transferred to 5 mL polystyrene tubes and centrifuged at 1000 rpm for 10 min. Next, supernatants were decanted, and the cells were incubated for 1 h at 4 °C with monoclonal antihuman SR-AI/MSR1-phycoerythrin (PE) antibody (clone 351615, R&D Systems) and APC antihuman CD36 antibody (clone: 5-271, Biolegend) or their corresponding isotype control APC mouse IgG2a, κ (clone: MOPC-173, Biolegend), and mouse IgG2B PE (clone 133303, R&D systems). Following antibody incubation, the cells were washed twice and then fixed with 1% PFA. CD36 APC and SRA-1 PE fluorescence was quantified via flow cytometry with a Gallios (Beckman Coulter) by collecting 10,000 events per sample and analyzed with Flow Jo software (Treestar) by quantifying the MFI of CD36 and SRA-1. A minimum of 3 experimental replicates were conducted for this study. All data were normalized to the basal condition. For microscopy, cells were washed with PBS and then blocked with 0.5% bovine serum albumin (BSA), 0.1% sodium azide, and 10% normal goat serum in PBS for 2 h. Next, cells were incubated for 3 h at 25 °C with monoclonal antihuman SR-AI/MSR1-phycoerythrin (PE) antibody (clone 351615, R&D Systems) and APC antihuman CD36 antibody (clone: 5-271, Biolegend) or their corresponding isotype control APC mouse IgG2a, κ (clone: MOPC-173, Biolegend), and PE mouse IgG2β (clone 133303, R&D systems). Following the incubation they were washed and then incubated with the secondary antibody, goat antimouse IgG2α alexa fluor 488 (SR-A1 conditions) or anti-mouse IgG2β alexa fluor 647 (CD36 conditions) for 1 h. They were then washed, fixed in 4% PFA, and counterstained with Hoechst 33342 before imaging on a Leica TCS SP2 confocal microscope. Representative images of CD36 and SRA receptor expression in HMDMs were obtained with ImageJ. The change in scavenger receptor expression was determined by the following equation:

$$\% \text{SR expression relative to oxLDL treatment} = 100 \times \frac{\text{SR MFI of treatment sample}}{\text{SR MFI of oxLDL only control sample}}$$

**Scavenger Receptor Gene Expression.** To evaluate the influence of NPs on scavenger receptor gene expression, HMDMs were incubated with unlabeled oxLDL (5 µg/mL)

with or without NPs of each chemistry in base media for 24 h. Following the incubation, treatment supernatants were removed and RNA was isolated with RNeasy Plus Mini Kit (Qiagen) according to the manufacturer's protocol. Reverse transcription was carried out using a High Capacity cDNA Reverse Transcription Kit (Applied Biosystems) following the manufacturer's protocol and performed in an Idaho Technology thermal cycler. Human SRA, CD36, and β-actin primers were designed by Harvard Primer Bank and synthesized by Integrated DNA Technology. Quantitative real-time polymerase chain reaction (qRT-PCR) was performed using Fast SYBR Green Master Mix (Applied Biosystems) per manufacturer's protocol in a LightCycler 480 (Roche Applied Science). Crossing points were determined using the second derivative maximum method in LightCycler 480 SW 1.5 software. Data is presented as a fold change calculated by ΔΔCt, using β-actin as the endogenous control gene and normalized to basal.

**Statistical Analysis.** Statistical analyses were performed using JMP by SAS. Statistical significance ( $p \leq 0.05$ ) was determined using a one-way ANOVA with Tukey's posthoc test for comparisons between multiple groups.

## RESULTS

**Effect of NP Shell and Core on the Inhibition of oxLDL Uptake in Macrophages.** NPs composed of bioactive shell ( $M_{12}$ PEG) and core ( $M_{12}$ ) components (Figure 1B), known to possess potent oxLDL inhibition activity, were fabricated and evaluated at an optimized concentration of  $1 \times 10^{-5}$  M (Supporting Information Figure 3A). As graded controls of bioactivity, additional NPs were designed and fabricated using differential amounts of nonbioactive shell ( $PS_{15}$ PEG) and core ( $PS_{14}$ ) components (Figure 1B). To discern the role of the core on NP bioactivity, NPs composed of a nonbioactive shell with different combinations of bioactive and nonbioactive cores were fabricated (top three rows of Figure 1C), and to discern the role of the shell on NP bioactivity and to identify synergies between the core and shell, NPs composed of a bioactive core with different combinations of bioactive and nonbioactive shells were fabricated (bottom three rows of Figure 1C). This enables one to deconstruct structure–activity relationships pertaining to the role of the shell versus core at inhibiting oxLDL uptake (Figure 2B). In this study, HMDMs were simultaneously exposed to both oxLDL and NPs, and the uptake of oxLDL was evaluated 24 h later via flow cytometry. The results in Figure 2B are from NPs composed of nonbioactive (100%  $PS_{15}$ PEG) shell formulated with different core combinations of bioactive  $M_{12}$  and nonbioactive  $PS_{14}$ , while Figure 2C represents NPs composed of a bioactive (100%  $M_{12}$ ) core formulated with different shell combinations of  $M_{12}$ PEG and nonbioactive  $PS_{15}$ PEG (all NP formulations evaluated are listed in Figure 1C). One can better understand the importance of the bioactive core,  $M_{12}$ , by comparing the change in oxLDL inhibition capacity of the nonbioactive shell NPs (100%  $PS_{15}$ PEG) as the content of  $M_{12}$  is increased and the content of  $PS_{14}$  is decreased within the core (Figure 2B), which resulted in a 2.8-fold increase in oxLDL uptake-inhibition capacity. However, one can evaluate the importance of the bioactive,  $M_{12}$ PEG, in the shell by comparing the change in oxLDL uptake-inhibition potential in Figure 2C of the bioactive core NPs (100%  $M_{12}$ ) as the shell  $PS_{15}$ PEG content is decreased and the  $M_{12}$ PEG content is increased (shifting from the 100%  $PS_{15}$ PEG shell to 100%  $M_{12}$ PEG shell formulations containing 100%  $M_{12}$ ), which resulted in a significant but smaller increase in inhibition

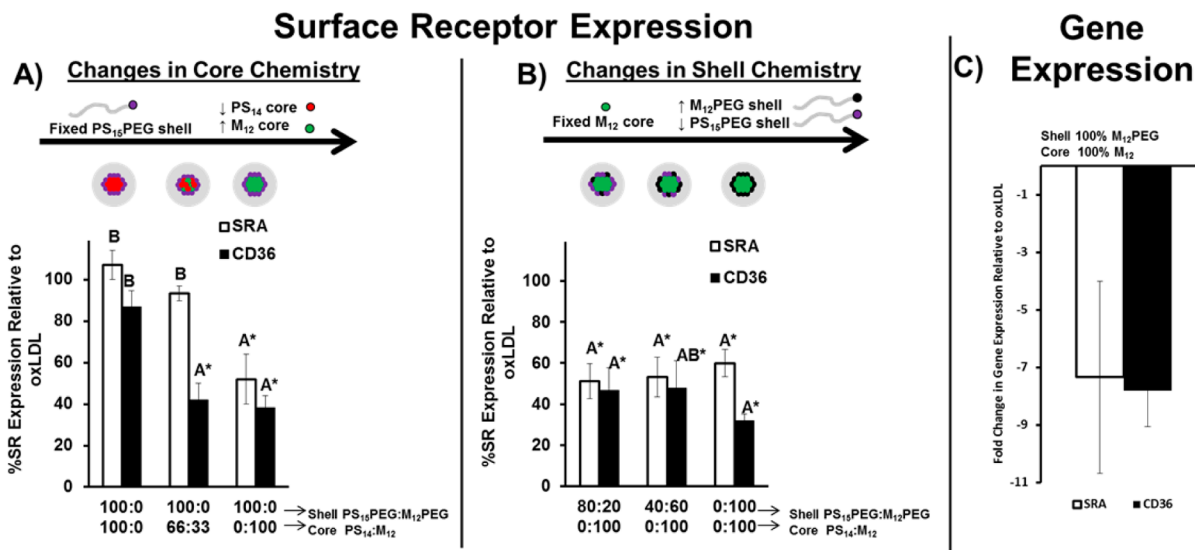


**Figure 4.** HMDMs exhibit NP influenced down-regulation of scavenger receptors, which is primarily regulated by the core, M<sub>12</sub>. (A,B) Protein-level surface expression of SRA and CD36 receptors was probed using flow cytometry analysis of HMDMs after 24 h incubation of NPs ( $1.5 \times 10^{-5}$  M) + oxLDL (5  $\mu$ g/mL) in the presence of 10% FBS. (A) NPs changing in the core chemistry are composed of a fixed -100% nonbioactive PS<sub>15</sub>PEG<sub>114</sub> shell formulated with differing core combinations of bioactive M<sub>12</sub> and nonbioactive PS<sub>14</sub>. (B) NPs changing in the shell chemistry and composed of a fixed 100% bioactive M<sub>12</sub> core formulated with differing shell combinations of M<sub>12</sub>PEG and nonbioactive PS<sub>15</sub>PEG<sub>114</sub>. Scavenger receptor expression (y-axis) is shown as a percent of the oxLDL control. C) Scavenger receptor gene expression was evaluated using q-RT-PCR analysis of HMDMs after 24 h incubation of NPs ( $1.5 \times 10^{-5}$  M) + oxLDL (5  $\mu$ g/mL) in the presence of 10% FBS. Data are from a minimum  $n = 3$  (error bars =  $\pm$ SEM). Statistical analysis was conducted over both parts A and B of this figure so comparisons can be made between all NP groups. Treatments with the same letter are not statistically significant from one another, and the asterisk (\*) indicates statistical significance from the oxLDL control. Statistical significance corresponds to  $p \leq 0.05$  for SRA and CD36 expression.

potential of 1.4-fold. Overall, all M<sub>12</sub>-core containing NP formulations resulted in a significant increase in inhibition potential from the oxLDL control. This was even observed with the nonbioactive 100% PS<sub>15</sub>PEG shell formulation, inhibiting 53% of oxLDL uptake. However, in this same shell formulation, when the bioactive, M<sub>12</sub>, core is replaced with 100% of the nonbioactive, PS<sub>14</sub> core, the oxLDL uptake-inhibition capacity drops markedly to 19%. This level of inhibition is not statistically significant from the oxLDL control. All NP formulations tested revealed to have no toxic effect on the HMDMs (Supporting Information Figure 1).

**Contribution of the NP Shell and Core to Scavenger Receptor Binding.** The ability of the NPs to inhibit oxLDL uptake in HMDMs as seen in Figure 2 may be due to competitive binding between the NPs and oxLDL to scavenger receptors. It is well documented that the unregulated uptake of oxLDL is primarily mediated through scavenger receptors such as SRA and CD36.<sup>1–4</sup> Thus, the ability of NPs to bind and be internalized by these receptors on HMDMs was evaluated. The results, presented in Figure 3B,C, demonstrate that M<sub>12</sub>-core containing NP formulations are internalized via SRA albeit with less internalization via CD36 (Supporting Information Table 1). However, it is interesting to note that NP internalization trends via SRA are similar to those via CD36. Between 44 and 59% internalization via SRA was observed for all formulations containing M<sub>12</sub>, but there was no statistical difference in internalization between any of these formulations. Changes in the shell composition did not appear to affect internalization via SRA as long as the M<sub>12</sub> core was present (Figure 3C). However, the formulation without a bioactive core or shell, 100% PS<sub>14</sub> core and 100% PS<sub>15</sub>PEG shell, resulted in very low overall cellular internalization (Supporting Information Figure 2) and especially via SRA (Figure 3B), which is why the

histograms in Figure 3D, for this formulation, appear at a lower fluorescence intensity. Significant NP internalization was only observed in the M<sub>12</sub> containing NP formulations (Supporting Information Figure 2). The ability of each NP formulation to be internalized via SRA is further represented in the histograms of Figure 3D,E in which the change in cellular fluorescence attributed to NP uptake via SRA can be identified by comparing the shift from the outlined histogram (NP uptake without SRA blocked) to the solid black histogram (NP uptake with SRA blocked). A further shift of the solid histogram to the left (lower MFI values) indicates a more pronounced effect of SRA blocking on NP uptake.

**Effect of NP Shell and Core on Scavenger Receptor Surface and Gene Expression.** The presence of scavenger receptors on the surface of plaque-resident macrophages is essential for the unregulated uptake of oxLDL molecules.<sup>1–4</sup> To examine the ability of the different NP formulations to mediate scavenger receptor expression on the surface of the HMDMs in the presence of modified lipids, the expression of SRA-1 (SRA isoform 1) and CD36 was evaluated after cotreatment with different NP formulations and oxLDL (Figure 4). All NP formulations containing 100% M<sub>12</sub> in the core engendered a pronounced decrease in the level of surface expression of SRA (40–49%) and CD36 (52–69%) as compared to the oxLDL control, Figure 4A,B. A trend can be observed in Figure 4A correlating the level of SRA and CD36 expression with the amount of M<sub>12</sub> in the NP core, with the expression of both scavenger receptors decreasing as the proportion of the M<sub>12</sub>-core composition was increased. As seen with SRA binding, the shell formulation did not have a significant effect on scavenger receptor expression if 100% M<sub>12</sub> core was present (Figure 4B). As to be expected, the formulation containing the 100% PS<sub>14</sub> core and 100% PS<sub>15</sub>PEG shell had a minimal effect on CD36

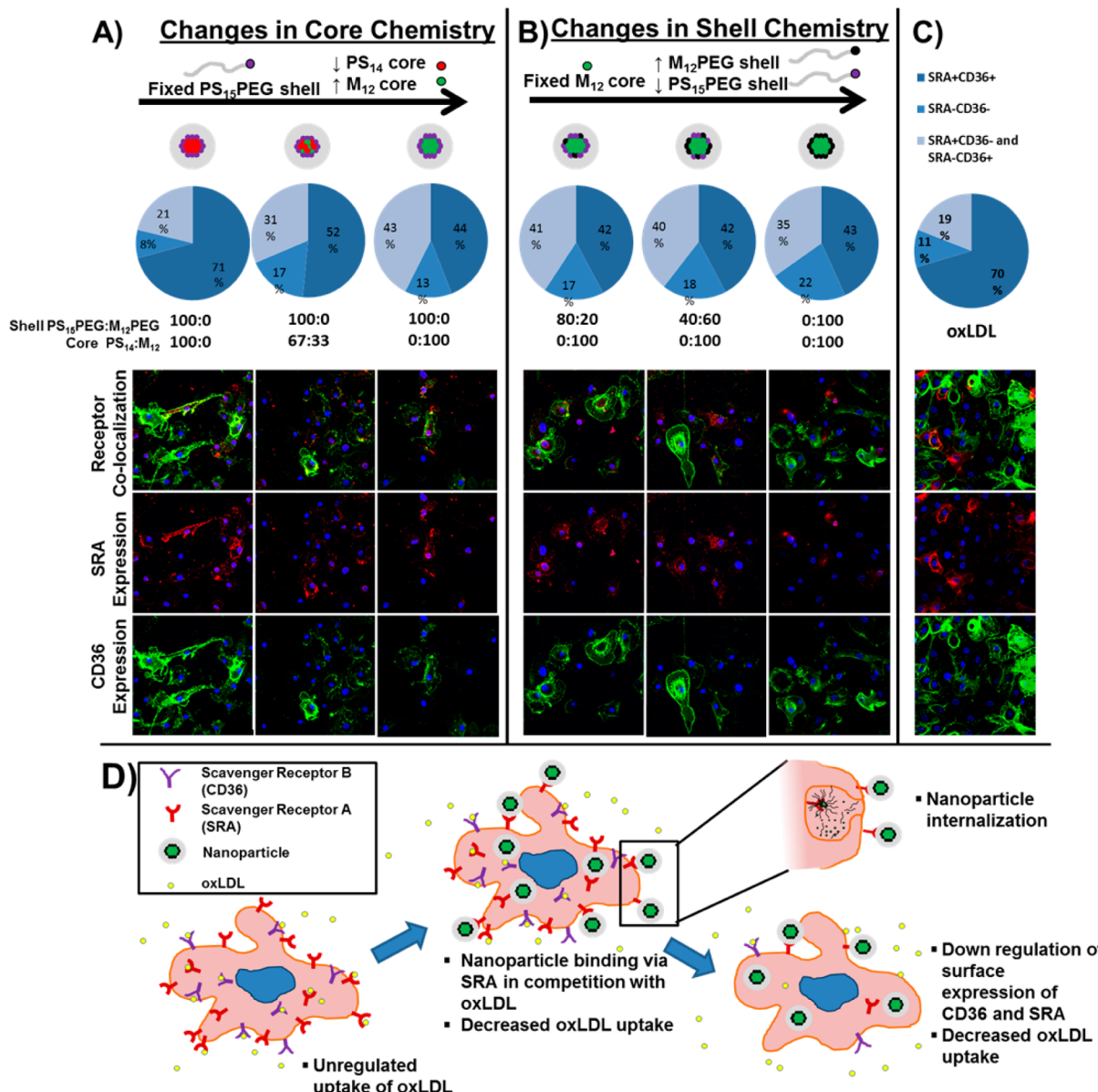


**Figure 5.** The most bioactive NPs shift the macrophage atherogenic phenotype from a population double positive for scavenger receptors (SRA<sup>+</sup>CD36<sup>+</sup>) to a population positive for only either scavenger receptor (SRA<sup>+</sup>CD36<sup>-</sup> and SRA<sup>-</sup>CD36<sup>+</sup>) or neither scavenger receptor (SRA<sup>-</sup>CD36<sup>-</sup>). Treatment groups include (A) NPs with varying core chemistry composed of a fixed 100% nonbioactive PS<sub>15</sub>PEG<sub>114</sub> shell formulated with differing core combinations of bioactive M<sub>12</sub> and nonbioactive PS<sub>14</sub>, (B) NPs with varying shell chemistry composed of a fixed 100% bioactive M<sub>12</sub> core formulated with differing shell combinations of M<sub>12</sub>PEG and nonbioactive PS<sub>15</sub>PEG<sub>114</sub>, and (C) oxLDL control. The HMDM scavenger receptor phenotypes presented in the top charts were obtained by flow cytometry, and below each chart are representative immunofluorescence micrographs for SRA and CD36 for each treatment group (SRA in red, CD36 in green, and cell nuclei in blue). Scavenger receptor surface expression was evaluated in HMDMs after 24 h incubation of NPs ( $1.5 \times 10^{-5}$  M) + oxLDL (5  $\mu$ g/mL) in the presence of 10% FBS. Flow cytometry data are from a minimum  $n = 3$ . (D) The proposed mechanism of action by which NPs inhibit oxLDL uptake in HMDMs. Atherosclerosis, influenced by the unregulated uptake of oxLDL, can potentially be inhibited with NP formulations that competitively bind scavenger receptors, become internalized, and cause a decrease in scavenger receptor surface expression, thus leading to a more sustained antiatherogenic phenotype in macrophages.

and SRA expression and was insignificant from the oxLDL control (Figure 4A). Consistent with surface expression, the 100% M<sub>12</sub>PEG shell 100% M<sub>12</sub> core NP formulation caused a down-regulation of mRNA gene expression of both receptors (Figure 4C).

A more in-depth assessment of the scavenger receptor phenotype of the HMDMs following NP treatment can be seen in Figure 5A,B and can be compared to the oxLDL control in Figure 5C. The dark blue area of the pie charts represent highly

atherogenic HMDMs that are positive for both SRA and CD36, whereas the lighter two shades of blue represent less atherogenic phenotypes, mid shade representing the population negative for both SRA and CD36, and the lightest shade of blue representing populations positive for only one scavenger receptor. Interestingly, the best NP inhibitor of oxLDL uptake, 100% M<sub>12</sub>PEG shell 100% M<sub>12</sub> core, caused a pronounced shift in scavenger receptor phenotypes by increasing the population of cells negative for both receptors (twice as many as the

oxLDL control) and decreasing the population of cells positive for both receptors (about half as many as the oxLDL control). Cells treated with NP formulations composed of 100% M<sub>12</sub> core demonstrated similar athero-protective scavenger receptor phenotypes (Figure 4B), whereas treatment with the non-bioactive 100% PS<sub>14</sub> core and 100% PS<sub>15</sub>PEG shell did not alter the HMDM phenotype from that observed with the oxLDL control (Figures 4A,C). Images representative of the changes in scavenger receptor expression for each treatment can be seen below each pie chart. While expression of SRA is much less intense than CD36, the images demonstrate that a larger population of the oxLDL and nonbioactive (100% PS<sub>14</sub> core and 100% PS<sub>15</sub>PEG shell) NP treated HMDMs are positive for both scavenger receptors versus the HMDMs treated with the M<sub>12</sub>-core containing formulations.

## ■ DISCUSSION

Management of the uncontrolled uptake of oxLDL by cells of actively developing atherosclerotic plaques, primarily macrophages, is a key target for therapeutic drug design and development.<sup>2</sup> Specifically, regulation of the scavenger receptor expression could be an effective strategy to prevent further accumulation of oxLDL and foam cell formation at the site of the atherosclerotic lesions. CD36 and SRA have been demonstrated to play a critical role in atherosclerotic lesion development, modified lipid accumulation, and foam cell formation in a cardiovascular disease mouse model.<sup>38</sup> Herein, we have fabricated a broad sublibrary of NPs to identify the critical macromolecular determinants for regulation of scavenger receptor-mediated mechanisms of foam cell formation and atherogenesis.

The fabrication of a range of NP formulations composed of bioactive and nonbioactive core and shell materials allowed us to discern the roles that the NP core and shell have on these major serial phenomena: SRA mediated-uptake and the regulation of scavenger receptor gene and surface expression, which together are able to repress the uptake of oxLDL. The proposed mechanism of action is depicted in Figure 5D. The core of the NP, composed of the bioactive M<sub>12</sub>, proved to be the most essential component for internalization via SRA and modulating the surface expression of scavenger receptors, SRA and CD36, causing a shift to a less atherogenic cellular phenotype (cells positive for neither or only one of the scavenger receptors vs cells positive for both). However, both the core and shell of the NP demonstrated importance in inhibiting oxLDL uptake, which suggests that they may have distinct yet significant mechanisms of bioactivity.

Upon evaluation of the bioactive shell, M<sub>12</sub>PEG, it is clear that it contributes further to the increase in oxLDL inhibition potential of the NP. However, changes in the shell bioactive component, M<sub>12</sub>PEG, do not appear to have an effect on the NP uptake via SRA or on the regulation of scavenger receptor expression. This suggests that the M<sub>12</sub>PEG shell, in the NP formulation with a M<sub>12</sub> core, is able to inhibit the uptake of oxLDL via alternate mechanisms. The M<sub>12</sub>PEG shell of the NP could allow for additional interactions with the cell (i.e., nonspecific binding to the lipid bilayer<sup>39</sup>), which would enable the NPs to occupy more of the cell surface and carry out additional oxLDL inhibition. Recent studies in our laboratories using lipid bilayers support this hypothesis of considerable membrane insertion by M<sub>12</sub>PEG.<sup>39</sup>

While the amphiphilic shell is integral for stabilization of the hydrophobic core and for enabling cellular interactions, one of

the striking new findings of this study is that the core material of the NP plays a more influential role on scavenger receptor-mediated uptake than the shell. The majority of the NP shell is composed of PEG, a material known to be nonfouling, thus limiting interaction with proteins.<sup>40</sup> The designated length of the PEG coating allows stable transport through physiological fluids but is short enough to allow for exposure of the hydrophobic and electrostatic charge associated with the core-PEG interface as it approaches the cellular membrane with cationic SRA residues. This would allow for electrostatic interactions between the negatively charged NP core and the positively charged surface scavenger receptors and/or the cellular membrane. Alternatively, as the NP approaches the cellular membrane, a portion of the M<sub>12</sub>PEG shell may partition from the NP to the cellular membrane exposing portions of the hydrophobic core. However, this interaction between cellular scavenger receptors and the NP core does not destabilize the NP based on recent work by York et al., who showed that the NPs remain intact with the shell and core components localized, soon after cellular binding and internalization.<sup>34</sup> This type of interaction (i.e., between the hydrophobic NP core and cell surface molecules) has been reported in the literature with some cell types having preferential attachment to hydrophobic polymers.<sup>41</sup> While we have demonstrated in this work that the NPs clearly interact with the HMDMs through SRA-mediated internalization, it is conceivable that there may be an extracellular interaction between the NPs, particularly serum-disrupted NPs, and the oxLDL. However, coincubation studies with NPs and oxLDL suggest that there was no detectable aggregation or increase in NP size (Supporting Information, Figure 3E). This is to be expected as the NPs are slightly negatively charged (as indicated by the zeta potential in Figure 1C) and have a PEG shell so any unimer interaction with highly oxidized oxLDL is unlikely since oxLDL itself is negatively charged.

Following scavenger receptor interactions, we hypothesize that the NPs are actively internalized, leading to continued downstream bioactive signaling including scavenger receptor down-regulation. While all M<sub>12</sub> core NPs were readily internalized via SRA, the NPs with more M<sub>12</sub> in the core demonstrated a stronger ability to lower cellular expression of CD36 and SRA, which was sustained for up to 48 h with the most bioactive formulation (Supporting Information Figure 3D). Not only did the M<sub>12</sub>-core formulations decrease the amount of scavenger receptors on the cell surface but the 100% M<sub>12</sub>PEG shell with 100% M<sub>12</sub> core formulation caused a doubling in the population of cells completely deficient of both key surface scavenger receptors. A shift of this magnitude in the scavenger receptor expression has not been reported before in human macrophages. It was confirmed that the surface receptor down-regulation is not just a factor of NP uptake and receptor depletion but is accompanied by, and is likely caused by, a decrease in the transcription of mRNA responsible for translation of these proteins. To further investigate the potential of NP interactions with oxLDL and this influence on NP bioactivity, scavenger receptor regulation was evaluated in the presence of only NPs. It was observed that scavenger receptor surface and gene expression were down-regulated in HMDMs; demonstrating that this effect is independent of oxLDL-NP interactions (Supporting Information Figure 3B,C). Furthermore, this 24 or 16 h NP preincubation in HMDMs served as a sufficient treatment to maintain inhibition of

subsequent oxLDL internalization (Supporting Information Figure 3B).

The NP uptake and down-regulation of cellular scavenger receptor expression correlates strongly with the inhibition of oxLDL uptake. Even with the NP formulation composed of the nonbioactive shell, PS<sub>15</sub>PEG, the presence of the M<sub>12</sub> core was able to increase oxLDL inhibition by 2.8-fold as compared to the nonbioactive PS<sub>14</sub> core. Such effects on scavenger receptor expression have been reported *in vitro* with smooth muscle cells and macrophages<sup>42,43</sup> and *in vivo* with hypercholesterolemic rabbits<sup>44</sup> following treatment with  $\alpha$ -tocopherol. The M<sub>12</sub> core NPs evaluated in this work appear to be functioning in a similar manner as  $\alpha$ -tocopherol; however, the signaling pathway that  $\alpha$ -tocopherol influences to down-regulate CD36 is largely unknown.<sup>42</sup> This consistent bioactivity may be due to the similarities in the chemical structures of  $\alpha$ -tocopherol and the lauroyl side chains of the M<sub>12</sub>, which may facilitate hydrophobic interactions. The ability of M<sub>12</sub> core NPs to alter scavenger receptor expression is possibly a concurrent effect of NP binding and blocking of scavenger receptors (providing a protective coating at the cell surface) and downstream intracellular effects including NP internalization and exposure to acidic vesicles in the macrophage. By binding scavenger receptors, the NPs would minimize interactions with oxLDL and disable downstream pathways, which lead to receptor replenishment. NPs that are internalized would likely encounter an enzyme rich environment, which may facilitate the release of M<sub>12</sub> from the NPs, enabling further disruption of receptor replenishment pathways. It is possible that the M<sub>12</sub> may be interfering with the reduction or phosphorylation of transcription factors responsible for upregulation of gene expression or with the PPAR $\gamma$ -dependent nuclear receptor signaling pathway responsible for scavenger receptor replenishment;<sup>37</sup> however, these mechanisms remain to be elucidated. Since oxLDL binding via CD36 has been shown to be a self-perpetuating cycle of unregulated uptake and receptor replenishment,<sup>4</sup> the proposed NP formulations could have two key concerted effects: the disruption of this cycle and a decrease in scavenger receptor access. Furthermore, cholesterol efflux has been linked to the decrease in CD36 expression,<sup>4</sup> again exemplifying the importance of scavenger receptor down-regulation for the management of atherosclerosis.

## CONCLUSIONS

We have advanced a new class of nanotherapeutics that can target macrophage scavenger receptors and repress the receptor atherogenic activity. We have identified the bioactive components of nanoparticles responsible for controlling expression of scavenger receptors, SRA and CD36, involved in the self-perpetuating cycle of unregulated oxLDL uptake and receptor replenishment. The hydrophobic core component of the NPs attenuated both the extracellular interactions of oxLDL with scavenger receptors and the intracellular events that further repress the uptake of oxLDL. A major finding of this study is the ability of bioactive nanoparticles to switch highly atherogenic macrophages to an athero-resistant phenotype, which could be the basis for the emergent design of nanomedicines targeted toward atherosclerotic plaques.

## ASSOCIATED CONTENT

### Supporting Information

Cell viability data. This material is available free of charge via the Internet at <http://pubs.acs.org>.

## AUTHOR INFORMATION

### Corresponding Author

\*(P.V.M.) Phone: 908-230-0147. Fax: 732-445-3753. E-mail: moghe@rutgers.edu.

### Notes

The authors declare no competing financial interest.

## ACKNOWLEDGMENTS

The authors would like to acknowledge the following financial support: National Heart, Lung and Blood Institute (R01HL107913 and R21HL93753 to P.V.M. and K.E.U.), the Coulter Foundation for Biomedical Engineering Translational Research Award (to P.V.M.), and NIH T32 training programs and fellowships (EB005583 to A.W.Y.; T32GM008339 to D.R.L.). The authors would like to thank Prof. John Anthony from the University of Kentucky, Department of Chemistry, Lexington, KY for the ETtPS.

## REFERENCES

- (1) Libby, P. Inflammation in atherosclerosis. *Nature* **2002**, *420*, 868–874.
- (2) Stephen, S. L.; Freestone, K.; Dunn, S.; Twigg, M. W.; Homer-Vanniasinkam, S.; Walker, J. H.; Wheatcroft, S. B.; Ponnambalam, S. Scavenger receptors and their potential as therapeutic targets in the treatment of cardiovascular disease. *Int. J. Hypertens.* **2010**, *2010*, 646929.
- (3) de Winther, M. P.; van Dijk, K. W.; Havekes, L. M.; Hofker, M. H. Macrophage scavenger receptor class A: A multifunctional receptor in atherosclerosis. *Arterioscler. Thromb. Vasc. Biol.* **2000**, *20*, 290–297.
- (4) Han, J.; Hajjar, D. P.; Tauras, J. M.; Nicholson, A. C. Cellular cholesterol regulates expression of the macrophage type B scavenger receptor, CD36. *J. Lipid Res.* **1999**, *40*, 830–838.
- (5) Collot-Teixeira, S.; Martin, J.; McDermott-Roe, C.; Poston, R.; McGregor, J. L. CD36 and macrophages in atherosclerosis. *Cardiovasc. Res.* **2007**, *75*, 468–477.
- (6) Nicholson, A. C.; Hajjar, D. P. CD36, oxidized LDL and PPAR gamma: pathological interactions in macrophages and atherosclerosis. *Vasc. Pharmacol.* **2004**, *41*, 139–146.
- (7) Geloen, A.; Helin, L.; Geeraert, B.; Malaud, E.; Holvoet, P.; Marguerie, G. CD36 inhibitors reduce postprandial hypertriglyceridemia and protect against diabetic dyslipidemia and atherosclerosis. *PLoS One* **2012**, *7*, e37633.
- (8) Wang, L.; Bao, Y.; Yang, Y.; Wu, Y.; Chen, X.; Si, S.; Hong, B. Discovery of antagonists for human scavenger receptor CD36 via an ELISA-like high-throughput screening assay. *J. Biomol. Screening* **2010**, *15*, 239–250.
- (9) Xu, Y.; Wang, J.; Bao, Y.; Jiang, W.; Zuo, L.; Song, D.; Hong, B.; Si, S. Identification of two antagonists of the scavenger receptor CD36 using a high-throughput screening model. *Anal. Biochem.* **2010**, *400*, 207–212.
- (10) Chnari, E.; Nikitczuk, J. S.; Uhrich, K. E.; Moghe, P. V. Nanoscale anionic macromolecules can inhibit cellular uptake of differentially oxidized LDL. *Biomacromolecules* **2006**, *7*, 597–603.
- (11) Chnari, E.; Nikitczuk, J. S.; Wang, J.; Uhrich, K. E.; Moghe, P. V. Engineered polymeric nanoparticles for receptor-targeted blockage of oxidized low density lipoprotein uptake and atherogenesis in macrophages. *Biomacromolecules* **2006**, *7*, 1796–1805.
- (12) Iverson, N. M.; Plourde, N. M.; Sparks, S. M.; Wang, J.; Patel, E. N.; Shah, P. S.; Lewis, D. R.; Zablocki, K. R.; Nackman, G. B.; Uhrich, K. E.; Moghe, P. V. Dual use of amphiphilic macromolecules as cholesterol efflux triggers and inhibitors of macrophage atherosclerosis. *Biomaterials* **2011**, *32*, 8319–8327.
- (13) Iverson, N. M.; Sparks, S. M.; Demirdirek, B.; Uhrich, K. E.; Moghe, P. V. Controllable inhibition of cellular uptake of oxidized low-density lipoprotein: structure-function relationships for nanoscale amphiphilic polymers. *Acta Biomater.* **2010**, *6*, 3081–3091.

- (14) Plourde, N. M.; Kortagere, S.; Welsh, W.; Moghe, P. V. Structure-activity relations of nanolipoblockers with the atherogenic domain of human macrophage scavenger receptor A. *Biomacromolecules* **2009**, *10*, 1381–1391.
- (15) Wang, L.; Bao, Y.; Yang, Y.; Wu, Y.; Chen, X.; Si, S.; Hong, B. Discovery of antagonists for human scavenger receptor CD36 via an ELISA-like high throughput screening assay. *J. Biomol. Screening* **2010**, *15*, 239–250.
- (16) Hehir, S.; Plourde, N. M.; Gu, L.; Poree, D. E.; Welsh, W. J.; Moghe, P. V.; Uhrich, K. E. Carbohydrate composition of amphiphilic macromolecules influences physicochemical properties and binding to atherogenic scavenger receptor A. *Acta Biomater.* **2012**, *8*, 3956–3962.
- (17) York, A. W.; Kirkland, S. E.; McCormick, C. L. Advances in the synthesis of amphiphilic block copolymers via RAFT polymerization: stimuli-responsive drug and gene delivery. *Adv. Drug Delivery Rev.* **2008**, *60*, 1018–1036.
- (18) Nishiyama, N.; Kataoka, K. Current state, achievements, and future prospects of polymeric micelles as nanocarriers for drug and gene delivery. *Pharmacol. Ther.* **2006**, *112*, 630–648.
- (19) Gaucher, G.; Dufresne, M. H.; Sant, V. P.; Kang, N.; Maysinger, D.; Leroux, J. C. Block copolymer micelles: preparation, characterization and application in drug delivery. *J. Controlled Release* **2005**, *109*, 169–188.
- (20) Bae, Y. H.; Yin, H. Stability issues of polymeric micelles. *J. Controlled Release* **2008**, *131*, 2–4.
- (21) Torchilin, V. P. Lipid-core micelles for targeted drug delivery. *Curr. Drug Delivery* **2005**, *2*, 319–327.
- (22) Allen, T. M.; Cullis, P. R. Drug delivery systems: entering the mainstream. *Science* **2004**, *303*, 1818–1822.
- (23) Ansell, S. M.; Johnstone, S. A.; Tardi, P. G.; Lo, L.; Xie, S.; Shu, Y.; Harasym, T. O.; Harasym, N. L.; Williams, L.; Bermudes, D.; Liboiron, B. D.; Saad, W.; Prud'homme, R. K.; Mayer, L. D. Modulating the therapeutic activity of nanoparticle delivered paclitaxel by manipulating the hydrophobicity of prodrug conjugates. *J. Med. Chem.* **2008**, *51*, 3288–3296.
- (24) Cabanes, A.; Briggs, K. E.; Gokhale, P. C.; Treat, J. A.; Rahman, A. Comparative in vivo studies with paclitaxel and liposome-encapsulated paclitaxel. *Int. J. Oncol.* **1998**, *12*, 1035–1040.
- (25) Chowdhary, R. K.; Shariff, I.; Dolphin, D. Drug release characteristics of lipid based benzoporphyrin derivative. *J. Pharm. Pharm. Sci.* **2003**, *6*, 13–19.
- (26) Liu, J.; Zeng, F.; Allen, C. Influence of serum protein on polycarbonate-based copolymer micelles as a delivery system for a hydrophobic anti-cancer agent. *J. Controlled Release* **2005**, *103*, 481–497.
- (27) Toncheva, V.; Schacht, E.; Ng, S. Y.; Barr, J.; Heller, J. Use of block copolymers of poly(ortho esters) and poly(ethylene glycol) micellar carriers as potential tumour targeting systems. *J. Drug Targeting* **2003**, *11*, 345–353.
- (28) Gindy, M. E.; Ji, S.; Hoye, T. R.; Panagiotopoulos, A. Z.; Prud'homme, R. K. Preparation of poly(ethylene glycol) protected nanoparticles with variable bioconjugate ligand density. *Biomacromolecules* **2008**, *9*, 2705–2711.
- (29) Gindy, M. E.; Panagiotopoulos, A. Z.; Prud'homme, R. K. Composite block copolymer stabilized nanoparticles: simultaneous encapsulation of organic actives and inorganic nanostructures. *Langmuir* **2008**, *24*, 83–90.
- (30) Gindy, M. E.; Prud'homme, R. K. Multifunctional nanoparticles for imaging, delivery and targeting in cancer therapy. *Expert Opin. Drug Delivery* **2009**, *6*, 865–878.
- (31) Johnson, B. K.; Prud'homme, R. K. Mechanism for rapid self-assembly of block copolymer nanoparticles. *Phys. Rev. Lett.* **2003**, *91*, 118302.
- (32) Kumar, V.; Adamson, D. H.; Prud'homme, R. K. Fluorescent polymeric nanoparticles: aggregation and phase behavior of pyrene and amphotericin B molecules in nanoparticle cores. *Small* **2010**, *6*, 2907–2914.
- (33) Kumar, V.; Hong, S. Y.; Maciag, A. E.; Saavedra, J. E.; Adamson, D. H.; Prud'homme, R. K.; Keefer, L. K.; Chakrapani, H. Stabilization of the nitric oxide (NO) prodrugs and anticancer leads, PABA/NO and Double JS-K, through incorporation into PEG-protected nanoparticles. *Mol. Pharmaceutics* **2010**, *7*, 291–298.
- (34) York, A. W.; Zablocki, K. R.; Lewis, D. R.; Gu, L.; Uhrich, K. E.; Prud'homme, R. K.; Moghe, P. V. Kinetically assembled nanoparticles of bioactive macromolecules exhibit enhanced stability and cell-targeted biological efficacy. *Adv. Mater.* **2012**, *24*, 733–739.
- (35) Adamson, D. H. Convenient method for the preparation of poly(ethylene oxide) and poly(ethylene oxide) block copolymers. *Abstr. Pap. Am. Chem. Soc.* **2000**, *220*, U273–U273.
- (36) Wolak, M. A.; Delcamp, J.; Landis, C. A.; Lane, P. A.; Anthony, J.; Kafafi, Z. High-performance organic light-emitting diodes based on dioxolane-substituted pentacene derivatives. *Adv. Funct. Mater.* **2006**, *16*, 1943–1949.
- (37) Steinberg, D. Low density lipoprotein oxidation and its pathobiological significance. *J. Biol. Chem.* **1997**, *272*, 20963–20966.
- (38) Febbraio, M.; Podrez, E. A.; Smith, J. D.; Hajjar, D. P.; Hazen, S. L.; Hoff, H. F.; Sharma, K.; Silverstein, R. L. Targeted disruption of the class B scavenger receptor CD36 protects against atherosclerotic lesion development in mice. *J. Clin. Invest.* **2000**, *105*, 1049–1056.
- (39) Martin, A.; Tomasini, M. D.; Gu, L.; Kholodovych, V.; Sommerfeld, S. D.; Uhrich, K. E.; Murthy, S.; Welsh, W. J.; Moghe, P. V. Biophysical characterization of novel amphiphilic macromolecules: modeling membrane interaction. *Langmuir* **2014**, to be submitted.
- (40) Ryan, S. M.; Mantovani, G.; Wang, X.; Haddleton, D. M.; Brayden, D. J. Advances in PEGylation of important biotech molecules: delivery aspects. *Expert Opin. Drug Delivery* **2008**, *5*, 371–383.
- (41) Hu, Y.; Xie, J.; Tong, Y. W.; Wang, C. H. Effect of PEG conformation and particle size on the cellular uptake efficiency of nanoparticles with the HepG2 cells. *J. Controlled Release* **2007**, *118*, 7–17.
- (42) Ricciarelli, R.; Zingg, J. M.; Azzi, A. Vitamin E reduces the uptake of oxidized LDL by inhibiting CD36 scavenger receptor expression in cultured aortic smooth muscle cells. *Circulation* **2000**, *102*, 82–87.
- (43) Teupser, D.; Thiery, J.; Seidel, D. Alpha-tocopherol down-regulates scavenger receptor activity in macrophages. *Atherosclerosis* **1999**, *144*, 109–115.
- (44) Ozer, N. K.; Negis, Y.; Aytan, N.; Villacorta, L.; Ricciarelli, R.; Zingg, J. M.; Azzi, A. Vitamin E inhibits CD36 scavenger receptor expression in hypercholesterolemic rabbits. *Atherosclerosis* **2006**, *184*, 15–20.